

Dual-Pipet Techniques for Probing Ionic Reactions

Biao Liu, Yuanhua Shao,[†] and Michael V. Mirkin*

Department of Chemistry and Biochemistry, Queens College—CUNY, Flushing, New York 11367

Novel dual-pipet electrodes prepared by pulling borosilicate θ -tubing are described. Three types of electrochemical experiments employing such devices include the following: (1) generation/collection experiments in which ions are ejected from one of two micropipets ("generator") into the external solution and collected at the second pipet ("collector"), (2) measurements of ohmic current–voltage curves, and (3) ion-transfer voltammetry "in the air". The first setup is used for probing ion transfers at the interface between two immiscible liquids and homogeneous reactions in solution involving ionic species. Such experiments are reported for two model processes, i.e., simple and facilitated transfers of potassium between aqueous and organic phases and complexation of potassium with dibenzo-18-crown-6 in organic solution. The second arrangement is used for characterization of θ -pipets. The last arrangement can be useful for preparation of gas sensors. The possibility of measuring the concentration of volatile substances (e.g., ammonia and nitric acid) in the gaseous phase has been demonstrated.

The main process in electrochemistry at the metal/solution interface is electron transfer (ET). Accordingly, numerous existing electrochemical methods found applications in studies of ET reactions and homogeneous processes coupled with a heterogeneous ET step.¹ Heterogeneous ion-transfer (IT) reactions are also common in electrochemical systems, e.g., polymer films, biological and artificial membranes, and chemically modified electrodes.² Unlike ET, these processes do not directly contribute to the electric current flowing at an electrode and, therefore, are less accessible to conventional electrochemical techniques. In contrast, electric current flowing at the interface between two immiscible electrolyte solutions (ITIES) is often due to IT reactions, and consequently, many methods of metal/liquid electrochemistry can be employed for studies of IT at the ITIES.³ However, fast

measurements at the ITIES (e.g., fast-scan cyclic voltammetry, short-time chronoamperometry, and pulse experiments) are problematic because of inherently high resistance and capacitance. Probing rapid IT and homogeneous reactions coupled with ion transfer at the ITIES is difficult.

The problems arising from uncompensated resistance and charging current can be diminished by placing one of two liquid phases in a micropipet to create a micro-ITIES.^{3a} Micropipet voltammetry introduced by Taylor and Girault⁴ has been successfully used to probe kinetics and thermodynamics of various IT processes.³ We recently showed the possibility of using even smaller, nanometer-sized, pipets for studies of very fast IT kinetics.⁵ However, micropipet techniques have not been widely employed for investigating multistep mechanisms involving IT and homogeneous ionic reactions. Although a vast literature concerning different types of ionic reactions (e.g., S_N2 -type processes,⁶ various organic transformations involving charged metal complexes,⁷ and ion binding to polyelectrolytes⁸ and DNA⁹) exists, relatively few electrochemical studies of such reactions have been reported.

Another alternative to fast perturbation measurements is using steady-state generation/collection (G/C) techniques. These methods, including well-known rotating ring–disk electrodes,¹⁰ closely spaced arrays of microelectrodes,¹¹ and scanning electrochemical microscopy (SECM),¹² have been successfully employed for studying complicated mechanisms and probing charge/mass transport in various media. The concept common for all these methods is generation of electroactive species at one electrode ("generator") and detection of the resulting flux at the second electrode ("collector"). Both generator (i_g) and collector (i_c) currents as well as collection efficiency (i.e., the ratio of two currents, $\eta = i_c/i_g$) can be used to investigate charge transport and chemical reactions occurring in the gap between two electrodes.

[†] Present address: Changchun Institute of Applied Chemistry, 159 People's St., Changchun 130022, Jilin Province, China.

(1) Bard, A. J.; Faulkner, L. R. *Electrochemical Methods*; Wiley: New York, 1980.
(2) (a) Koryta, J. *Ions, electrodes and membranes*, 2nd ed.; Wiley & Sons: New York, 1992. (b) Murray, R. W. In *Electroanalytical Chemistry*; Bard, A. J., Ed.; Marcel Dekker: New York, 1984; Vol. 13, p 191. (c) Inzelt, G. In *Electroanalytical Chemistry*; Bard, A. J., Ed.; Marcel Dekker: New York, 1994; Vol. 18, p 89.
(3) (a) Girault, H. H. In *Modern Aspects of Electrochemistry*; Bockris, J. O'M., Conway, B. E., White, R. E., Eds.; Plenum Press: New York, 1993; Vol. 25, p 1. (b) Samec, Z.; Kakiuchi, T. In *Advances in Electrochemical Science and Electrochemical Engineering*; Gerischer, H., Tobias, C. W., Eds.; VCH: New York, 1995; Vol. 4, p 297. (c) Samec, Z. In *Liquid–Liquid Interfaces. Theory and Methods*; Volkov, A. G., Deamer, D. W., Eds.; CRC Press: Boca Raton, 1996. (d) Benjamin, I. *Chem. Rev.* **1996**, 96, 1449.

(4) Taylor, G.; Girault, H. H. *J. Electroanal. Chem.* **1986**, 208, 179.
(5) Shao, Y.; Mirkin, M. V. *J. Am. Chem. Soc.* **1997**, 119, 8103.
(6) (a) Shaik, S. S.; Schlegel, H. B.; Wolfe, S. *Theoretical Aspects of Physical Organic Chemistry. The S_N2 Mechanism*; Wiley-Interscience: New York, 1992. (b) Marcus, R. A. *J. Phys. Chem. A* **1997**, 101, 4072.
(7) Harman, W. D. *Chem. Rev.* **1997**, 97, 1953.
(8) Ciszowska, M.; Osteryoung, J. G. *J. Phys. Chem. B* **1998**, 102, 291.
(9) Horrocks, B. R.; Mirkin, M. V. *Anal. Chem.* **1998**, 70, 4653.
(10) Albery, W. J.; Hitchman, M. L. *Ring-Disc Electrodes*; Calrendon: Oxford, 1971.
(11) (a) Chidsey, C. E. D.; Feldman, B. J.; Lundgren, C.; Murray, R. W. *Anal. Chem.* **1986**, 58, 601. (b) Varco Shea, T.; Bard, A. J. *Anal. Chem.* **1987**, 59, 2101. (c) Licht, S.; Cammarata, V.; Wrighton, M. S. *J. Phys. Chem.* **1990**, 94, 6133. (d) Tatistcheff, H. B.; Fritsch-Faules, I.; Wrighton, M. S. *J. Phys. Chem.* **1993**, 97, 2732. (e) Fosset, B.; Amatore, C. A.; Bartelt, J. E.; Michael A. C.; Wightman, R. M. *Anal. Chem.* **1991**, 63, 306.
(12) Bard, A. J.; Fan, F.-R. F.; Mirkin, M. V. In *Electroanalytical Chemistry*; Bard, A. J., Ed.; Marcel Dekker: New York, 1994; Vol. 18, p 243.

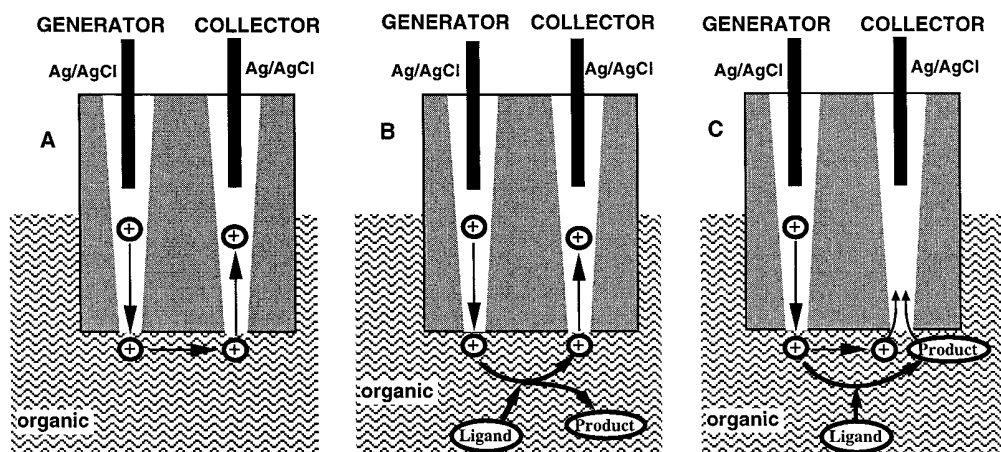
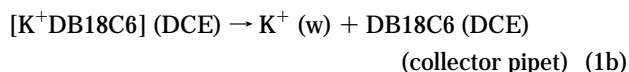
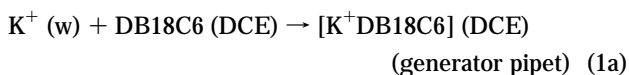


Figure 1. Probing ionic reactions with a dual-pipet device. (A) Simple transfer of a cation, (B, C) IT is followed by a chemical reaction in solution. (B) The reaction product is not transferred into the collector pipet. (C) Both the cation and the reaction product are collected.

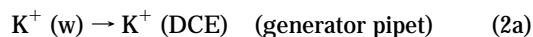
In a recent communication, we introduced an electrochemical G/C technique for studying ionic reactions that involve no oxidation/reduction steps.¹³ Such experiments were carried out using dual-pipet (or θ -pipet) electrodes. A θ -pipet consists of two micrometer- or submicrometer-sized pipets (usually filled with aqueous solutions) separated by a submicrometer-thick band of glass. In a simple IT experiment, one of the pipets ("generator") contains a cation (or an anion) that can be transferred to the outer (usually organic) solution by biasing this pipet at a positive potential, E_g , with respect to the external reference electrode. A significant fraction of ejected cations reach the negatively biased second pipet ("collector") and get transferred back into the aqueous phase (Figure 1A). If the collector potential (E_c) is sufficiently negative for the transfer reaction to be controlled by diffusion, the collection efficiency reaches its maximum value, which is determined by device geometry and is essentially independent of E_g .¹³

An ion ejected from the generator pipet may participate in a homogeneous chemical reaction. When such a reaction affects the collection efficiency, its kinetics and/or thermodynamics can be probed. If the reaction product does not contribute to the collector current (i.e., either it cannot be transferred into water or its diffusion coefficient is too small), the collection efficiency decreases with increasing rate of coupled homogeneous reaction (Figure 1B). If the reaction product is charged and can be transferred to water (Figure 1C), the collector voltammogram consists of two waves occurring at different potentials and corresponding to the product and cation transfers. A number of metal ion complexation reactions belong to the latter class, e.g., potassium transfer from water into 1,2-dichloroethane (DCE) facilitated by dibenzo-18-crown-6 (DB18C6)

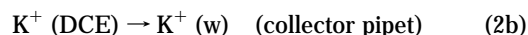


The facilitated transfer of potassium to DCE expressed by eq 1a occurs at significantly less positive potentials than a simple

transfer of K^+



Conversely, the reverse transfer of potassium from DCE into the aqueous phase via interfacial dissociation (reaction 1b) occurs at significantly more negative E_c than the simple transfer (reaction 2b)



Here, we use this model experimental system to show the possibility of quantitative separation of different IT processes from each other and from the transfer of supporting electrolyte and explore the possibility of mechanistic analysis of a complex process using θ -pipets.

Using a dual-pipet device one also can perform measurements in a thin liquid film formed on the surface of glass separating two pipets. In this way, voltammetry can be carried out "in the air", i.e., in the absence of the external liquid macrophase. Three different possibilities are outlined in Figure 2. In Figure 2A one of the pipets (e.g., a generator) is filled with an aqueous solution and the second one (e.g., a collector) with an organic solution. An ion ejected from the generator pipet can travel through the liquid film and be transferred into the collector pipet. This process is driven by external voltage applied between two internal reference electrodes inserted into the θ -pipet. Alternatively, two barrels of the θ -pipet can be filled with the same phase (e.g., organic) and separated by a thin film of the second (e.g., aqueous) phase acting as a liquid membrane (Figure 2B).

Finally, a dual-pipet device can be used as a sensor for water-soluble (or organic) gaseous species that can change the composition and ionic conductivity of the thin liquid layer (Figure 2C). Amperometric measurements at solid electrodes "in air", i.e., without bulk solution phase, have been reported earlier.¹⁴ The presence of a thin liquid film on the electrode surface is essential

(14) (a) Brina, R.; Pons, S.; Fleischmann, J. *Electroanal. Chem.* **1988**, *244*, 81. (b) Fang, Y.; Leddy, J. J. *Electroanal. Chem.* **1995**, *384*, 5. (c) Mossier-Boss, P. A.; Lieberman, S. H. *J. Electroanal. Chem.* **1999**, *460*, 105. (d) Fan, F.-R. F.; Bard, A. J. *Science* **1995**, *270*, 1849.

(13) Shao, Y.; Liu, B.; Mirkin, M. V. *J. Am. Chem. Soc.* **1998**, *120*, 12700.

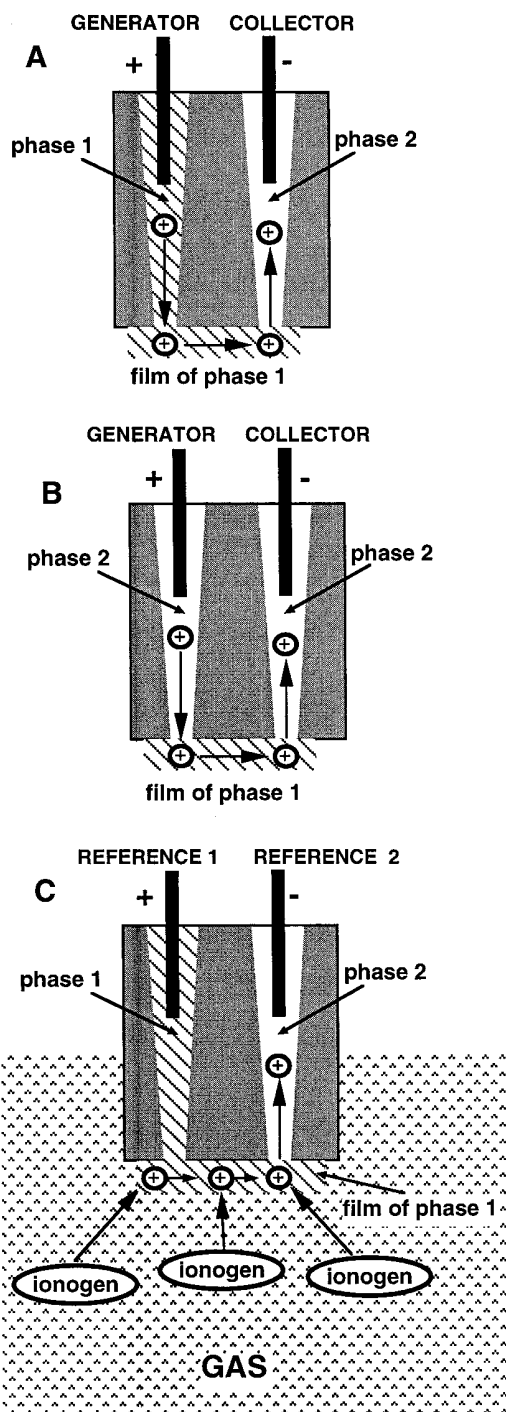


Figure 2. Voltammetry "in air" (A, B) and gas sensing (C) using θ -pipets.

for such measurements.^{14b} Because the liquid films spontaneously forming on solid electrode surfaces are extremely thin and resistive,^{14d} the obtained voltammograms were poorly shaped and distorted by resistive potential drop. A somewhat thicker and less resistive film linking two barrels of the θ -pipet yields higher quality voltammetric response suitable for qualitative and quantitative analytical determinations.

EXPERIMENTAL SECTION

Chemicals. Tetrahexylammonium perchlorate (THAClO₄) and LiCl from Johnson Matthey (Ward Hill, MA), MgCl₂ from Fisher

(Fair Lawn, NJ), dibenzo-18-crown-6 from PCR Research Chemicals (Gainesville, FL), 1,2-dichloroethane (99.8% HPLC grade), tetrabutylammonium chloride (TBACl), potassium tetrakis(4-chlorophenyl)borate (KTPBCl) and KCl from Aldrich (Milwaukee, WI) and trimethylchlorosilane (Hüls America, Inc., Bristol, PA) were used as received. Tetrabutylammonium tetrakis(4-chlorophenyl)borate (TBATPBCl) was prepared as described previously¹⁵ and served as a supporting electrolyte for the organic phase. All aqueous solutions were prepared from deionized water (Milli-Q, Millipore Corp.).

Instrumentation. The EI-400 bipotentiostat (Ensmann Instruments, Bloomington, IN) was employed to control the potentials of two pipets serving as working electrodes with respect to the organic reference electrode and record cyclic voltammograms. Voltammograms "in air" were obtained using a BAS 100B electrochemical workstation (Bioanalytical Systems, West Lafayette, IN). All prepared pipets were inspected before measurements using an Olympus BH2 optical microscope ($\times 100$ – $\times 1000$ magnification).

Pipets and Electrochemical Cells. Dual-pipet electrodes were made from borosilicate θ -tubing (OD = 1.5 mm, Sutter Instrument Co.) using a Sutter model P-2000 laser-based puller. The shape of a pulled θ -pipet is determined by the choice of laser puller parameter values. These values are specific for a given puller: i.e., two different pullers of the same type (e.g., P-2000) may require significantly different programs to produce similar pipets. Moreover, the performance of each puller changes slightly with time, so the pulling program has to be modified. Hence it is impossible to specify a program that would allow reproducible fabrication of pipets with the desired properties. Such a program has to be found by a trial-and-error method. A proper choice of pulling parameters yielded two very similar closely spaced pipets. Unless there is a special need for two halves of the θ -pipet to be different, the similarity of the two radii is advantageous because the symmetry of the device can somewhat simplify the data analysis. Since the ohmic resistance of a pipet is largely determined by the length of the narrow shaft leading to the orifice,^{5,16a} a pulling program was developed to produce short (patch-type) pipets. Both the orifice radii and the thickness of the pipet wall were measured microscopically.

The pipets were filled with either aqueous or organic solutions from the back using a small (10–25 μ L) syringe. A 0.125 mm silver wire coated with either AgCl (aqueous filling solution) or AgTPBCl (organic filling solution) was inserted into each pipet from the back.

The outer glass wall was silanized to prevent the formation of an aqueous film between two pipets and mixing of the filling solutions. This was done by dipping the pipet tip into trimethylchlorosilane for 1–2 min while the flow of argon (sufficiently fast to produce small bubbles) was passed through the pipet from the back to avoid silanization of the inner wall of a pipet. This was crucial because the outer organic solvent gets drawn inside a pipet if its inner surface is hydrophobic.¹⁷

(15) Shao, Y.; Girault, H. H. *J. Electroanal. Chem.* **1990**, 282, 59.

(16) (a) Stewart, A. A.; Taylor, G.; Girault, H. H.; McAleer, J. J. *J. Electroanal. Chem.* **1990**, 296, 491. (b) Beattie, P. D.; Delay, A.; Girault, H. H. *J. Electroanal. Chem.* **1995**, 380, 167.

(17) Shao, Y.; Mirkin, M. V. *Anal. Chem.* **1998**, 70, 3155.

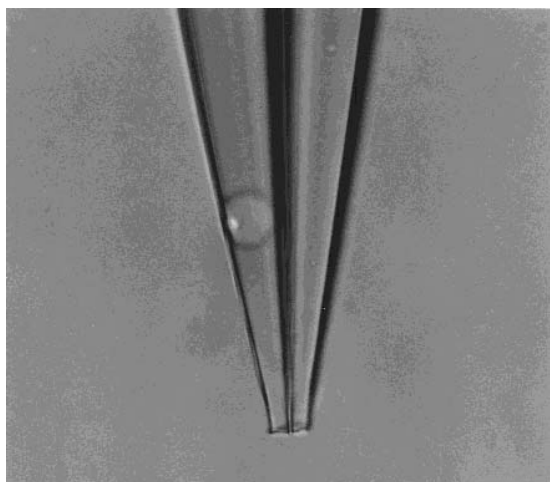


Figure 3. Photomicrograph of the θ -pipet filled with an aqueous solution. A thin ($\leq 1 \mu\text{m}$ thick) glass wall separates two barrels, one of which is blocked by an air bubble. Both orifices are $\sim 4.5 \mu\text{m}$ radius.

Voltammetric experiments with micropipets were carried out in a 5 mL vial inside a Faraday cage. Using a bipotentiostat, the voltage was applied between the reference electrode inside each barrel of the θ -pipet and the reference electrode in the outer solution. All experiments were carried out at room temperature ($25 \pm 2^\circ\text{C}$).

Voltammetry in the Gaseous Phase. Voltammetric experiments without external solution were carried out using a θ -pipet with one barrel filled with an aqueous solution and the second barrel filled with organic phase. In a two-electrode setup, voltage was applied between Ag/AgCl and Ag/AgTPBCl reference electrodes inserted in two barrels. The glass surface was not silanized, and the pipet orifices were linked by a thin aqueous film formed on the outer pipet wall.¹⁷ In this arrangement, water sometimes flows into the second barrel and forms a micrometer-thick aqueous layer, which can be seen microscopically. Such pipets have been discarded. Only dual pipets with no detectable amount of water inside the second barrel were employed in our experiments. Thus the liquid/liquid interface was confined to the orifice of the organic-filled capillary.

To measure concentrations of gaseous compounds, a θ -pipet was introduced in a 20 mL vial through its airtight stopper. The vial contained a ~ 2 mL solution of a volatile substance (e.g., ammonia or nitric acid), and the distance between the pipet tip and the solution surface was ~ 1 cm. Several voltammograms were recorded during a few minute period. The experiment was carried out until the pipet response stabilized, so the successive voltammograms were virtually identical. Then the pipet was introduced in the next vial containing a higher concentration of the substance of interest.

RESULTS AND DISCUSSION

Characterization of θ -Pipets. Similarly to conventional, single-barrel pipets, the size and shape of θ -pipets can be changed by varying the pulling parameters. In particular, the radius of each of two orifices can be either on a micrometer or a submicrometer scale. If the device is micrometer-sized, it can be characterized by optical microscopy. The θ -pipet in Figure 3 has two similar

micrometer-sized apertures separated by a submicrometer-thick glass wall. An air bubble trapped in one of the barrels can be removed by gently knocking on the outer wall. Unlike single-barrel pipets whose orifice is typically disk-shaped, the apertures of a dual pipet look like two halves of an ellipse separated by a very thin line of glass. An advantage of such a geometry compared to a more symmetrical group of two coplanar disks is a somewhat higher collection efficiency.¹³ However, simulating mass transfer in such a system is challenging, and no exact theory is currently available for θ -pipets.

Two main objectives of electrochemical characterization of a dual pipet are to determine the effective radii and to check that each of two pipets can be independently polarized. The radius of each orifice can be evaluated from an IT voltammogram obtained at one pipet while the second one is disconnected. As discussed previously,¹⁷ the diffusion limiting current to a water-filled single pipet with a sufficiently thick, silanized outer wall can be calculated from eq 3 where D and c respectively are the diffusion coefficient

$$i_d = 4nFaDc \quad (3)$$

and concentration of species in the outer solution responsible for the interfacial charge-transfer reaction, a is the effective radius of the pipet orifice, F is the Faraday constant, and n is the transferred charge. The effective radius values calculated from eq 3 for both halves of the θ -pipet must be close to the values found from optical microscopy.

Similarly to single pipets,¹⁷ the outer surface of a water-filled dual pipet has to be silanized to prevent formation of an aqueous film. Such a film can short-circuit the θ -pipet by connecting its two halves. In the absence of a surface aqueous layer, the currents flow between each of two pipets and the external reference electrode. In contrast, when the liquid film connects two orifices, the current flows directly from one pipet to the other. Two simple experiments allowing the distinction between these two cases were carried out using the model reaction of facilitated potassium transfer. The generator and collector pipets were as follows:

Cell 1

(generator)

Ag/AgTPBCl/ x mM DB18C6 + 10 mM TBATPBCl//
outer DCE solution

20 mM KCl/AgCl/Ag
generator pipet

(collector)

Ag/AgTPBCl/ x mM DB18C6 + 10 mM TBATPBCl//
outer DCE solution

10 mM MgCl_2 /AgCl/Ag
collector pipet

In the first experiment, both pipets are initially biased at the same potential (with respect to the external reference) at which no appreciable current flows at either pipet. Then the potential of the generator pipet (E_g) is scanned in a positive direction to induce ejection of potassium ions, while the collector potential (E_c) is kept constant (Figure 4). In the absence of an aqueous surface layer, two voltammograms, i.e., steady-state generator (curve 1

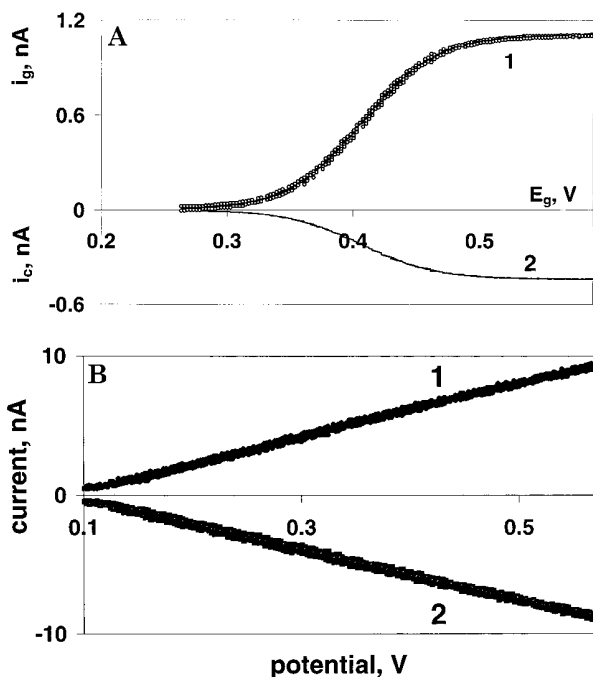


Figure 4. (A) Generator (1) and collector (2) voltammograms of the transfer of K^+ between water and DCE containing DB18C6 obtained in cell 1. Solid line in curve 1 is the generator voltammogram reconstructed from the i_c vs E_g data as described in the text. (B) i_g vs E_g and i_c vs E_g curves obtained with an aqueous film linking two barrels of the θ -pipet. E_c was (A) 0.25 and (B) 0.1 V vs AgTPBCl. DCE contained 1 mM DB18C6. (B) the collector pipet contained 10 mM LiCl instead of $MgCl_2$. Generator potential was swept at (A) 20 and (B) 100 mV/s. For other parameters, see cell 1.

in Figure 4A) and collector (curve 2) voltammograms, are obtained as described in ref 13. In contrast, if the water film links two pipets, positive (generator) and negative (collector) currents of exactly the same magnitude are observed in an analogous experiment (Figure 4B). The current–voltage curves are linear because the current is controlled by resistance between two Ag/AgCl electrodes rather than by the interfacial IT rate. The large current represents the flow of supporting electrolyte between two pipets. The complete resistance of the generator/aqueous film/collector system calculated from Figure 4B using Ohm's law, $R = 67\text{ M}\Omega$. Subtracting from this value the doubled value of the resistance of a $\sim 5\text{ }\mu\text{m}$ diameter pipet filled with 0.01 M aqueous electrolyte ($\sim 10\text{ M}\Omega^{16b}$), one can evaluate the resistance of the aqueous layer to be $\sim 50\text{ M}\Omega$. Since the width of the aqueous film (i.e., the distance between two orifices) is $\leq 1\text{ }\mu\text{m}$, such a high ohmic resistance indicates that the layer is only a few nanometers thick.

Another way to detect the short circuit is by sweeping the potential of one of the pipets while the second pipet is disconnected from the potentiostat. When the surface film is present, the voltammograms obtained in this way are practically identical for both pipets. This can be expected because both curves are produced by IT across the same interface (i.e., the interface between the aqueous film and DCE) and the filling solutions in two barrels are mixed. In contrast, when no aqueous film is present on the outer pipet wall, the collector voltammogram is flat and featureless because this pipet contains no transferable ion.

Probing Ion-Transfer and Homogeneous Ionic Reactions.

Typical generator and collector voltammograms of potassium transfer (see cell 1) are shown in Figure 4A. As discussed earlier,¹³ the steady-state sigmoidal waves in both voltammograms are due to facilitated transfer of K^+ into DCE (curve 1, generator current is due to reaction 1a) and the reverse reaction (curve 2, collector current is due to reaction 1b). As expected, the i_g is limited by diffusion of DB18C6 in DCE as long as its concentration, c_{DB18C6} , is much lower than the potassium concentration inside the generator pipet (in Figure 4A, $c_{\text{DB18C6}} = 1\text{ mM}$ and $c_{\text{KCl}} = 20\text{ mM}$). The pipet radius calculated from the limiting current ($5\text{ }\mu\text{m}$) was in agreement with the value found by optical microscopy. A more accurate radius value ($4.8\text{ }\mu\text{m}$) was determined from the slope of limiting current vs c_{DB18C6} of the linear plot. As expected, this dependence was strictly linear with a practically zero intercept.

When only one IT process occurs at a generator pipet and the transferred species do not participate in any homogeneous reaction, the collection efficiency, η , is essentially independent of E_g .¹³ In this case, η is determined by collector potential and device geometry and is independent of i_g . Thus, one can measure the maximum value of η (η_{max}) when all ions reaching the opening of the collector pipet are transferred into it. The η_{max} is a constant characteristic for a given θ -pipet. Consequently, it should be possible to reconstruct the generator voltammogram from an i_c vs E_g dependence. For an uncomplicated IT reaction with diffusion-controlled collection, the generator current at any E_g can be calculated as

$$i_g = i_c / \eta_{\text{max}} \quad (4)$$

An example of such a reconstruction is shown in Figure 4A, where the generator voltammogram (curve 1, solid line) was calculated from the collector voltammogram (curve 2) using eq 4 with $\eta_{\text{max}} = 0.396$. A perfect agreement between calculated and measured i_g values (solid line and symbols) proves the validity of the reconstruction. A similar procedure is useful for more complicated processes in which more than one IT reaction contribute to the i_g , and the analysis of generator voltammograms is difficult. If only one kind of ion is collected, eq 4 gives the component of the generator current produced by transfer of this ion.

Two concurrent IT reactions can be separated as shown in Figure 5. The simple transfer of potassium from water to DCE (reaction 2a) occurs at a positively biased generator pipet simultaneously with the transfer of TPBCl⁻ into the aqueous filling solution (see cell 1 with $c_{\text{DB18C6}} = 0$)

$$i_g = i_{g,K^+} + i_{g,TPBCl^-} \quad (5)$$

Unlike the generator voltammogram (curve 1 in Figure 5), which is produced by two different IT reactions and consequently is hard to analyze, a collection voltammogram (curve 2) is only due to the transfer of K^+ from DCE to water. At a low scan rate (e.g., $v = 20\text{ mV/s}$ in Figure 5) this quasi-steady-state curve is sigmoidal. One can use eq 4 with $\eta_{\text{max}} = 0.31$ determined independently for the employed θ -pipet to calculate the flux of K^+ ejected from the generator (i_{g,K^+}) as a function of E_g (i.e., $i_{g,K^+} = i_c / \eta_{\text{max}}$; curve 3 in Figure 5). The subtraction of i_{g,K^+} from the

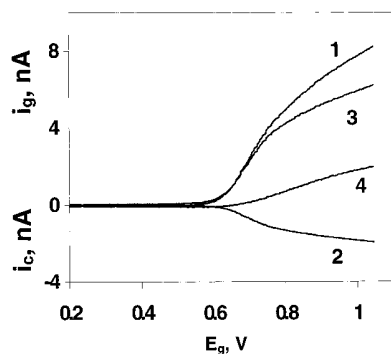


Figure 5. Separation of two concurrent IT processes. Generator voltammogram (curve 1) is produced by simultaneously occurring transfers of K^+ and $TPBCl^-$. The flux of K^+ ejected from the generator pipet (curve 3) was obtained from the collection current of K^+ (curve 2) using eq 4. The transfer current of $TPBCl^-$ (curve 4) was obtained by subtraction of curve 3 from curve 1. $E_c = 0.15$ V vs $AgTPBCl$. $c_{DB18C6} = 0$. For other parameters, see Figure 4A.

original voltammogram (i.e., the subtraction of curve 3 from curve 1) yields the $TPBCl^-$ transfer current at the generator orifice (curve 4). This current is produced by steady-state convergent diffusion of $TPBCl^-$ to a micrometer-sized generator pipet. Despite error produced by subtraction, this voltammogram is retraceable and sigmoidal. One should notice that the half-wave potential of $TPBCl^-$ transfer is ~ 100 mV more positive than the $E_{1/2}$ of potassium transfer. To our knowledge, this is the first direct observation of the $TPBCl^-$ transfer wave. The overlap of voltammetric waves of alkali metal transfers and those of hydrophobic anions (e.g., $TPBCl^-$) has previously hindered kinetic studies of these reactions.¹⁸ Using the G/C setup, one can quantitatively separate these processes and probe them independently. Significantly smaller θ -pipets, which can provide the high mass-transfer rates required for measurements of rapid IT kinetics, are currently been developed.

A more complicated combination of several IT processes with a homogeneous ionic reaction can be observed when potassium transfer is conducted in the presence of DB18C6 and a large positive potential is applied to the generator pipet. If $c_{DB18C6} \ll c_{KCl}$, the generator current is produced by two IT processes, i.e., facilitated transfer of potassium by DB18C6 (reaction 1a) and simple transfer of K^+ (reaction 2a) (at $E_g < \sim 0.9$ V the transfer of $TPBCl^-$ can be neglected):

$$i_g = i_{g,KDB18C6} + i_{g,K^+} \quad (6)$$

The collector current in this case consists of two components

$$i_c = i_{c,KDB18C6} + i_{c,K^+} \quad (7)$$

where the $i_{c,KDB18C6}$ term represents interfacial dissociation (reaction 1b) and i_{c,K^+} corresponds to simple transfer of potassium (reaction 2b). Figure 6 contains a generator voltammogram (curve 1) and two corresponding i_c vs E_g curves obtained at $E_c = 0.25$

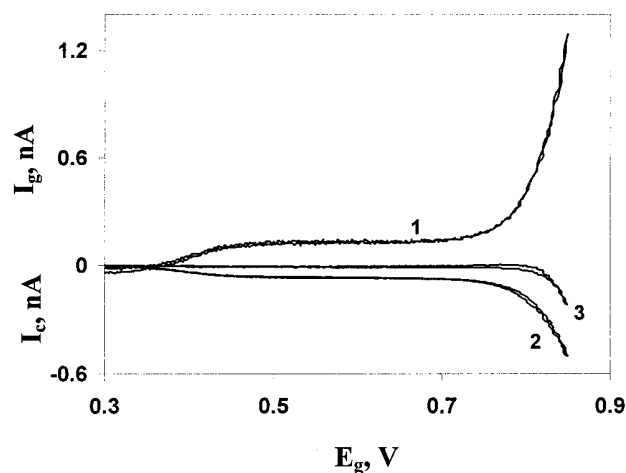
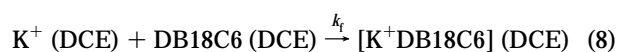


Figure 6. Analysis of IT coupled with a homogeneous ion complexation reaction. Generator voltammogram (1) of the transfer of potassium from the aqueous solution into DCE containing 0.25 mM DB18C6 and corresponding background-subtracted collector curves obtained at $E_c = 0.25$ (2) and 0.6 V vs $AgTPBCl$. The shape of the generator voltammogram was practically independent of E_c . Collector pipet contained 0.01 M $LiCl$. For other parameters, see cell 1.

(curve 2) and 0.6 V (curve 3) with $c_{KCl} = 20$ mM, $c_{DB18C6} = 0.25$ mM, and $c_{TPBCl^-} = 10$ mM. Since $c_{KCl} \gg c_{DB18C6}$, the i_g at positive E_g is much higher than the diffusion current of crown ether to the generator pipet ($i_{g,KDB18C6}$), which appears as a small wave at $E_g \sim 0.4$ V.

The collector voltammograms in Figure 6 are different because at $E_c = 0.25$ V both complexed and uncomplexed forms of potassium are collected, while only uncomplexed K^+ is collected at $E_c = 0.6$ V ($i_c = i_{c,K^+}$ because the interfacial dissociation of $[K^+DB18C6]$ at this potential is slow). Accordingly, a small steady-state wave corresponding to reaction 1b can be seen in curve 2 but not in curve 3. One might expect the difference between two collector voltammograms to be equal to the height of that wave, but the actual difference between those curves at positive E_g is much larger. Apparently, K^+ ejected from the generator pipet at more positive E_g participate in homogeneous complexation reaction with DB18C6 in DCE



At $E_c = 0.25$ V (but not at 0.6 V), potassium from $[K^+DB18C6]$ species produced by both interfacial and homogeneous complexation reactions can be transferred into the collector pipet. Therefore, the difference between curves 2 and 3 ($= i_{c,KDB18C6}$) represents the total amount of $[K^+DB18C6]$ species produced via reactions 1a and 8 that reach the collector orifice. At high positive E_g , the magnitude of $i_{c,KDB18C6}$ is limited by one of three factors: (i) the diffusion of K^+ inside the generator pipet, (ii) the rate of reaction 8, and (iii) the diffusion of DB18C6 to the θ -pipet.

If the diffusion of K^+ were rate-limiting (assumption i), the collection efficiency would be independent of crown ether concentration in DCE. The data in Table 1 illustrate the effect of c_{DB18C6} at different collector potentials (i.e., $E_c = 0.25$ or 0.6 V). As expected, with no complexing agent present in DCE the same $\eta_{max} = 0.37$ was measured at both E_c values. At $E_c = 0.25$ V (at

(18) (a) Samec, Z.; Marecek, V.; Colombini, M. P. *J. Electroanal. Chem.* **1988**, 257, 147. (b) Shao, Y.; Stewart, A. A.; Girault, H. H. *J. Chem. Soc., Faraday Trans.* **1991**, 87, 2593. (c) Stewart, A. A.; Shao, Y.; Pereira, C. M.; Girault, H. H. *J. Electroanal. Chem.* **1991**, 305, 135.

Table 1. Effect of DB18C6 Concentration on Collection Efficiency of Potassium in Cell 1 at Different Collection Potentials; $E_g = 0.85$ V. $\eta_{\max} = 0.37$

c_{DB18C6} (mM)	collection efficiency	
	$E_c = 0.25$ V	$E_c = 0.6$ V
0	0.38	0.37
0.10	0.35	0.30
0.25	0.35	0.17
0.50	0.36	0.07
1.0	0.37	0.03

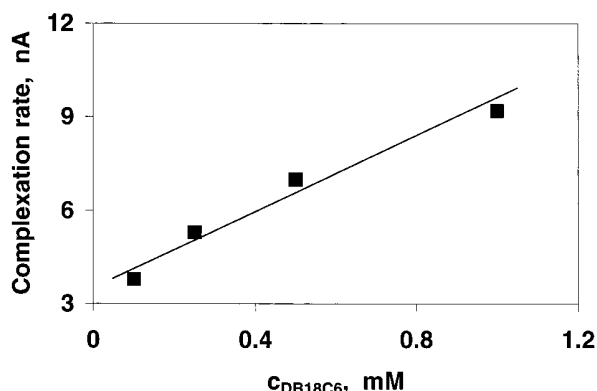


Figure 7. Dependence of the homogeneous complexation rate (eq 9) on c_{DB18C6} .

which both complexed and uncomplexed forms of potassium are collected), the collection efficiency is essentially independent of c_{DB18C6} . However, at $E_c = 0.6$ V, η decreases markedly with increasing c_{DB18C6} . The η vs c_{DB18C6} dependence in Table 1 is essentially linear. This is consistent with the diffusion-limited complexation rate (assumption ii). The limiting diffusion flux of DB18C6 in this case is not the flux to the generator orifice but rather to the entire tip area of the θ -pipet (the effective radius of the θ -pipet at the tip was ~ 3 times the radius of the generator aperture). This flux is sufficiently large to account for the amount of $[\text{K}^+\text{DB18C6}]$ arriving to the collector pipet. The rate of reaction 8 can be evaluated from the difference between i_c values at $E_c = 0.25$ V and $E_c = 0.6$ V, which represents the total amount of complexed potassium arriving to the collector. Dividing this quantity by collection efficiency, one gets an estimate for the total complexation rate in the system. To evaluate homogeneous complexation rate, the contribution of interfacial complexation (i.e., $i_{g,\text{KDB18C6}}$) has to be subtracted

$$\text{homogeneous complexation rate} = [i_c(0.25 \text{ V}) - i_c(0.6 \text{ V})]/\eta_{\max} - i_{g,\text{KDB18C6}} \quad (9)$$

Figure 7 shows that complexation rate is a linear function of c_{DB18C6} , as one would expect for a diffusion-controlled reaction. However, the linear dependence in Figure 7 does not go through the origin because of the approximate nature of eq 9.

Table 2 contains the results of G/C experiments carried out with a different θ -pipet in which the separation distance between two orifices was much larger. Hence the $\eta_{\max} = 0.17$ is much smaller than the maximum collection efficiency in Table 1 (0.37). However, the concentration effect is qualitatively similar, i.e., at

Table 2. Effect of DB18C6 Concentration on Collection Efficiency of Potassium in Cell 1 at Different Collection Potentials^a

c_{DB18C6} (mM)	collection efficiency	
	$E_c = 0.25$ V	$E_c = 0.6$ V
0	0.17	0.17
0.10	0.16	0.10
0.25	0.17	0.034
0.50	0.17	0.018
1.0	0.17	0.006

^a The spacing between two pipet apertures is much larger than in Table 1. $E_g = 0.7$ V. $\eta_{\max} = 0.17$.

$E_c = 0.25$ V, the η is essentially independent of c_{DB18C6} , and at $E_c = 0.6$ V, it decreases with increasing c_{DB18C6} .

To explore the possibility of measuring the kinetics of reaction 8, we carried out G/C experiments with $c_{\text{KCl}} \ll c_{\text{DB18C6}}$ (e.g., $c_{\text{KCl}} = 0.2$ mM, $c_{\text{DB18C6}} \geq 0.5$ mM). Under these conditions, the concentration of DB18C6 near the pipet is essentially constant, independent of i_g , and equal to the bulk value (c_{DB18C6}). Reaction 8 can be considered as a pseudo-first-order process whose rate is

$$\text{rate} = k c_{\text{K}^+}^s = k_f c_{\text{DB18C6}} c_{\text{K}^+}^s \quad (10)$$

where $c_{\text{K}^+}^s$ is the average concentration of K^+ at the θ -pipet surface proportional to i_g and $k = k_f c_{\text{DB18C6}}$ is the effective first-order rate constant (s^{-1}). If the kinetics of complexation reaction are rate-limiting, the collection efficiency of uncomplexed potassium for a given pipet (i.e., η at $E_c = 0.6$ V) should be determined by a single dimensionless parameter, $\kappa = ka^2/D$.¹⁹ Moreover, the η value measured at $E_c = 0.6$ V should decrease with increasing c_{DB18C6} . But at $c_{\text{KCl}} < c_{\text{DB18C6}}$ the measured η values were very low ($< 1\%$) and practically independent of c_{DB18C6} . This indicates that homogeneous complexation of potassium ions by DB18C6 in DCE is too fast to be measured using micrometer-sized dual pipets. According to ref 19, the lower limit for the dimensionless rate constant of reaction 8 is $\kappa \sim 10$, which corresponds to $k \gtrsim 500 \text{ s}^{-1}$ or $k_f \gtrsim 10^6 \text{ M}^{-1} \text{ s}^{-1}$. These numbers represent the upper limit for the determinable complexation rate constant for the current configuration. Smaller (nanometer-sized) pipets are required for probing rapid complexation reactions.

Ion-Transfer Voltammetry "in Air". In the G/C experiments described above, one has to eliminate the liquid film that spontaneously forms on the outer glass surface and connects two halves of the θ -pipet. The same film can be used to perform different types of electrochemical experiments which can be called voltammetry in air, i.e., with no external liquid macrophase. Several possible arrangements include the following: (i) one pipet filled with an aqueous solution, the second filled with organic phase, and either aqueous or organic film between (Figure 2A); (ii) both pipets filled with either water or organic phase and a thin film of an immiscible solvent between them (Figure 2B). In this paper, only the first arrangement will be discussed. Since the outer surface of the θ -pipet was not silanized, the gap between two pipets was covered with an aqueous film.

(19) Phillips, C. G.; Stone, H. A. *J. Electroanal. Chem.* **1997**, 437, 157.

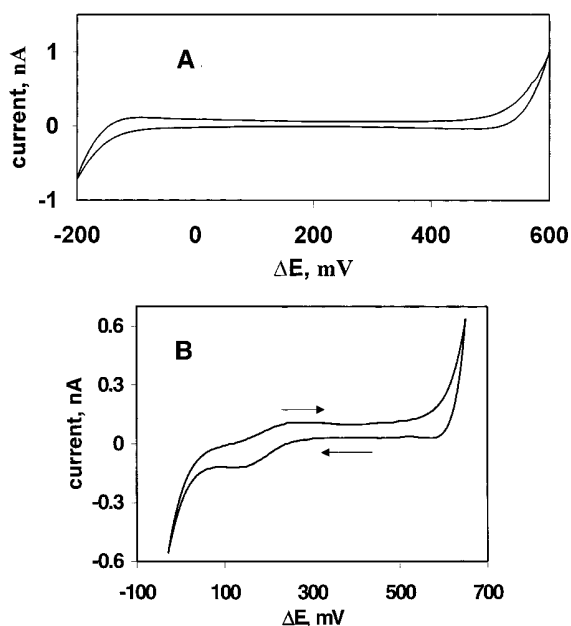


Figure 8. Voltammetry "in the air". Background voltammogram (A) and a voltammogram of facilitated potassium transfer (B) obtained by application of voltage between two reference electrodes in cell 2. (B) DCE contained 0.25 mM DB18C6; the aqueous solution contained 20 mM KCl. Arrows indicate the potential sweep direction. $v = 20$ mV/s. The radii of two orifices are 5.5 (water-filled pipet) and $4.5 \mu\text{m}$ (DCE-filled pipet).

Figure 8A shows a typical cyclic voltammogram obtained by application of voltage ($\Delta E = E_{\text{Ag/AgCl}} - E_{\text{Ag/AgTPBCl}}$) across the θ -pipet containing only supporting electrolyte (i.e., 0.01 M TBATPBCl in DCE and 0.01 M LiCl in water):

Cell 2

Ag/AgCl/10 mM LiCl//10 mM TBATPBCl/AgTPBCl/Ag
water-filled pipet DCE-filled pipet

This curve is similar to a conventional voltammogram which could be obtained with a single water- or organic-filled pipet immersed in an immiscible external solution.³ The only significant difference is a much wider potential window (i.e., the difference between the onset of TBA⁺ ejection from the pipet and Li⁺ transfer. The window width is ~ 700 mV for a θ -pipet vs ~ 500 mV for a single pipet). This difference is caused by the resistive potential drop in the aqueous film covering the gap between two barrels. From the $iR \sim 200$ mV and the current of the order of 1 nA, the calculated resistance is $\sim 200 \text{ M}\Omega$, which is significantly larger than the resistance of a θ -pipet immersed in DCE. This indicates that the aqueous surface film may be thinner and more resistive in the absence of external solvent.

A well-defined IT cyclic voltammogram in Figure 8B was obtained after addition of 0.25 mM DB18C6 to the organic filling solution and replacement of LiCl with KCl in the water-filled pipet. While steady-state concentration profiles are formed in the thin aqueous film connecting two barrels, no full equilibration between this film and the bulk liquids inside pipets can be expected (this would require a long-range diffusion impossible at the experi-

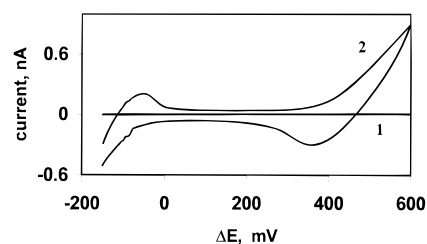


Figure 9. Effect of the exposure of θ -pipet to ammonia vapor on the resistance of the aqueous film covering the gap between two barrels. (1) The pipet is in the air. The current is too small to be seen on the scale of curve 2. (2) The same pipet is exposed to a 1 M solution of ammonia. $v = 100$ mV/s. The radii of the two orifices are 1 (water-filled pipet) and $1.5 \mu\text{m}$ (DCE-filled pipet). See cell 2 for solution compositions.

mental time scale). The solution gap works as a tiny (perhaps fL) microreactor in which the processes involving minuscule amounts of reagents can be probed. An example of such measurements is presented in the next section.

θ -Pipets as Gas Sensors. The response of a θ -pipet "in air" is largely determined by the properties of the aqueous surface layer, and it is very sensitive to changes in film composition. Such changes occur when the pipet is exposed to a soluble gas. Thus, IT voltammetry at a θ -pipet can be used for detection and quantification of gaseous substances. A small ratio of the film thickness to its surface area should result in a high sensitivity and fast response time of such a sensor.

Two detection modes can be used with θ -pipets, i.e., conductivity and IT. In the former case, the concentration of charge carriers in the surface layer increases upon exposure to soluble gas. Figure 9 shows two voltammograms obtained with the same θ -pipet (cell 2) exposed to air (curve 1) and ammonia vapors (curve 2). As discussed above, the apparent potential window is extended by resistive effect, and the IT current in curve 1 is very low. In contrast, the large currents produced by transfers of TBA⁺ from DCE to water (at negative ΔE) and Li⁺ from water to DCE (at positive ΔE) in curve 2 indicate that absorbed ammonia caused a significant decrease in the film resistance. One should notice that the wave of ammonium transfer cannot be seen within the potential window in this experiment. The presence of NH₃ in the gaseous phase is detected by increasing transfer of supporting electrolyte and significantly higher charging current in the middle of the potential window. These currents are directly proportional to the solution conductivity which, in turn, is proportional to ionic concentration (the response may also have been affected by increasing pH as discussed below). Thus, the current flowing at a given potential depends strongly on ammonium concentration in the surface layer, and a θ -pipet can be used for monitoring relative concentration of ammonia in the gaseous phase. To measure absolute values of NH₃ concentration, the pipet sensor has to be calibrated.

Alternatively, the concentration of a gaseous compound can be found from the transfer current of an ion generated in the liquid film by species absorbed from the gaseous phase. For example, NH₄⁺ formed in the aqueous layer when the θ -pipet is exposed to ammonia vapor can be transferred to DCE. This reaction can be facilitated by DB18C6 (Figure 10A)

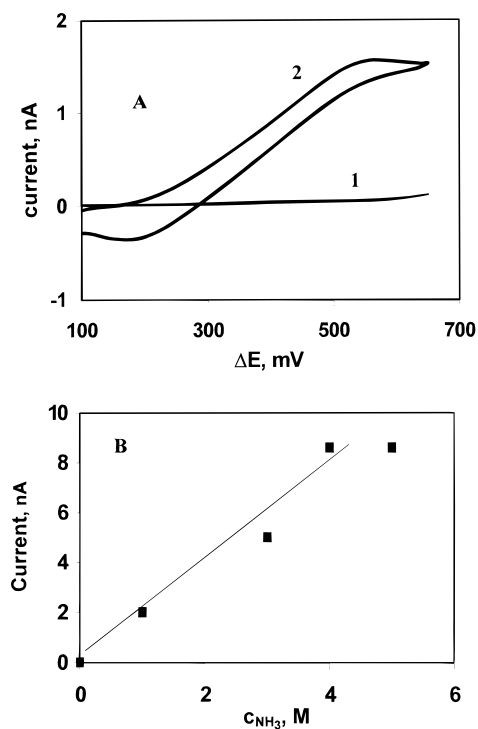
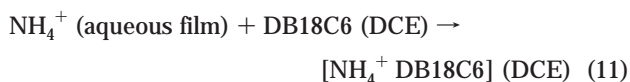


Figure 10. Detection of ammonia in the air. (A) Cyclic voltammograms obtained with a θ -pipet (cell 2 with 20 mM DB18C6 added to DCE) exposed to air (1) and ammonia vapor above its 2 M solution (2). (B) Dependence of voltammetric current at $\Delta E = 0.56$ V on concentration of NH_3 in the vapor-generating solution. $v = 20$ mV/s. The radii of the two orifices are 3 (water-filled pipet) and $1.5 \mu\text{m}$ (DCE-filled pipet).



The blank (background) curve obtained in the absence of ammonium ion (curve 1) is similar to one in Figure 8A. The wave of NH_4^+ appears immediately after the pipet is introduced in a vial containing ammonia vapor above its concentrated solution. The shape of the wave changes during next several minutes and then the response becomes stable and reproducible (curve 2 in Figure 10A). This time most probably reflects the dynamics of ammonia vaporization in a closed vial since the equilibration in a submicrometer-thick aqueous layer should be rapid. The wave of facilitated transfer (reaction 11) is sigmoidal while the reverse wave is peak-shaped. This means that the forward reaction is limited by convergent diffusion of NH_4^+ in the aqueous film to the orifice of the DCE-containing pipet. In contrast, the reverse peak is due to essentially linear diffusion of the $[\text{NH}_4^+ \text{DB18C6}]$ complex inside the pipet containing DCE solution. Although the voltammogram is somewhat drawn out because of high film resistance, the diffusion limiting current is not affected by resistive potential drop and can be used for analytical determinations. The partial pressure of ammonia above the solution is expected to be proportional to its concentration when the latter is not very high. The diffusion limiting IT current measured at $\Delta E = 0.56$ V applied to cell 2 increases linearly with concentration of ammonia in the vapor-generating solution at moderate c_{NH_3} values (Figure 10B). At $c_{\text{NH}_3} > 4$ mol/L, the current vs concentration dependence

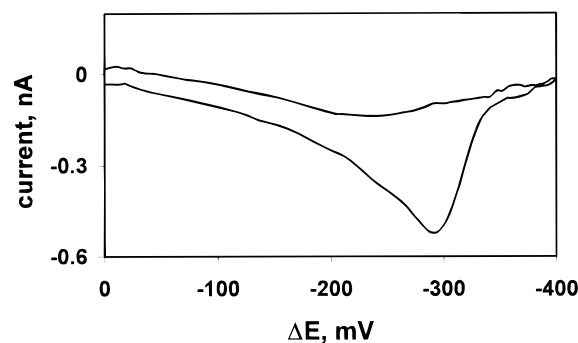


Figure 11. Background-subtracted voltammogram of nitrate transfer obtained with a θ -pipet (cell 2) exposed to a 1 M solution of nitric acid. $v = 20$ mV/s.

levels off. This saturation may be caused by different reasons, e.g., deviations from Henry's law at high concentrations or extensive ion pairing inside the aqueous layer covering glass surface.

One should notice that the amount of analyte accumulated in the θ -pipet during described measurements is very small. In ~ 10 min after the pipet is removed from the ammonium atmosphere, "blank" voltammograms practically indistinguishable from curve 1 in Figure 10A could be obtained. Thus, the same pipet can be employed for a number of measurements or for continuous monitoring of a gaseous analyte. One also can use such a sensor for remote measurements of the concentration of a volatile solute in a liquid phase (i.e., without an electrochemical probe having to contact it).

Another example of IT-based sensing of a gaseous substance is shown in Figure 11. In this experiment, nitrate was accumulated in the aqueous film by exposing a dual pipet to HNO_3 vapor. In this case, TBA^+ was replaced with THA^+ in the organic supporting electrolyte, so that nitrate ion transfer from water to DCE occurred within the potential window. The voltammogram of nitrate transfer is peak-shaped and not as well defined as the one in Figure 10A. Moreover, the pipet seems to be more resistive, the wave is less stable, and its height decreases with time. One of possible reasons for these differences is that absorption of HNO_3 makes the aqueous surface layer acidic while the exposure to NH_3 results in basic pH. The ion migration in the aqueous surface film is somewhat similar to capillary electrophoresis because a voltage drop of ~ 200 mV across a submicrometer gap between two orifices creates a large electric field. Since the film is only nanometers thick, the double-layer effect should be very important.²⁰ This effect, in turn, depends on pH, which can affect the charge of the underlying glass surface.²⁰ The electrophoretic and electroosmotic mobilities of cationic NH_4^+ and anionic NO_3^- should also be different.

The conductivity-based detection of gaseous substances is more general than IT measurements because most soluble gases can affect film resistivity, but not all of them can be transferred across the ITIES. The advantages of IT detection include selectivity and somewhat higher sensitivity. The surface liquid layer in all pipets used in this work was aqueous, and only the detection of water-soluble gases was discussed. However, the detection of

(20) Wei, C.; Bard, A. J.; Feldberg, S. W. *Anal. Chem.* **1997**, *69*, 4627.

organic compounds in the gas phase may also be possible using a θ -pipet with a nonaqueous sensing film.

CONCLUSIONS

We have described electrochemical characterization of and voltammetric experiments with θ -pipet electrodes. Such a device consisting of two closely spaced micropipets is produced by pulling θ -shaped glass tubing. Voltammetric response of a dual pipet depends strongly on the extent of hydrophilicity of its outer surface. When a glass pipet is immersed in an organic solvent, its hydrophilic outer wall retains a submicrometer-thick aqueous layer. If both barrels of the pipet are filled with an aqueous solution, the surface water film links them producing a short circuit. The aqueous layer can be eliminated by silanizing the outer pipet wall to render it hydrophobic. The developed diagnostic procedures allow one to evaluate the adequacy of silanization.

Generation/collection measurements employing θ -pipets were used for probing charge-transfer processes at the liquid/liquid interface and homogeneous ionic reactions. Using this technique, concurrent IT reactions occurring at the ITIES can be quantitatively separated and the kinetics of homogeneous reactions involving ionic species can be probed. The upper limit for the determinable bimolecular rate constant is $\sim 10^6 \text{ M}^{-1} \text{ s}^{-1}$ with currently available micrometer-sized pipets. Although this was not

enough for measurements of rapid complexation of K^+ by DB18C6, it may be possible to probe other ionic reactions such as binding of cations to DNA and polyelectrolytes. The fabrication of smaller θ -pipets will enable investigation of faster reactions and detection of short-lived intermediates.

Another mode of measurements is voltammetry "in air" in which a θ -pipet is not immersed in any external solvent and IT occurs in the nanometer-thick film of solvent linking its two barrels. This film acts as a microreactor and can be used to detect and quantitate various gaseous substances. In this way, IT voltammograms of NH_4^+ and NO_3^- were obtained when a pipet was exposed to vapors of ammonia and nitric acid, and linear dependence of the voltammetric response on concentration of vapor-generating solution has been demonstrated.

ACKNOWLEDGMENT

The support by the donors of the Petroleum Research Fund administered by the American Chemical Society and a grant from PSC-CUNY are gratefully acknowledged.

Received for review July 14, 1999. Accepted November 3, 1999.

AC990771P